

# Modeling the Mechanical Behavior of Vertebral Trabecular Bone: Effects of Age-Related Changes in Microstructure

M. J. SILVA<sup>1</sup> and L. J. GIBSON<sup>2</sup>

<sup>1</sup> Orthopaedic Research Laboratory, Department of Orthopaedic Surgery, Washington University School of Medicine, St. Louis, MO, USA

<sup>2</sup> Department of Materials Science and Engineering, Massachusetts Institute of Technology, Cambridge, MA, USA

Age-related reductions in the thickness and number of trabeculae in vertebral trabecular bone have been documented by several workers, yet the relative effects of these changes on mechanical properties are not known. We developed a two-dimensional model of human vertebral trabecular bone and investigated its mechanical behavior using finite element analysis. The stress-strain behavior, failure mode, and strain distributions predicted using the model were consistent with those observed for vertebral trabecular bone under compressive loading. Random reductions in the *number* of trabeculae reduced the modulus and strength of the models two to five times more than uniform reductions in the *thickness* of trabeculae that caused the same loss of bone volume. For example, randomly removing longitudinal trabeculae to achieve a reduction in density of 10% reduced the strength by approximately 70%, whereas removing the same amount of bone by uniformly reducing the thickness of the longitudinal trabeculae only reduced the strength by approximately 20%. For a simulation of aged bone, in which the thickness and number of trabeculae were reduced concurrently, the strength was 23% of its intact (“young”) value. When the bone mass of the aged model was restored to its intact level by increasing the thickness but not the number of trabeculae, the strength increased by 60%, but was still only 37% of its intact value. These combined findings, based on a two-dimensional, idealized model of vertebral trabecular bone, illustrate the importance of maintaining trabecular number and suggest that it may not be possible to restore bone strength following a period of advanced bone loss if a substantial number of trabeculae have been resorbed. Thus, until treatments exist that can increase trabecular number, the most effective treatment strategy is to prevent the degradation of bone strength by maintaining the number of trabeculae at a healthy level. (Bone 21:191–199; 1997) © 1997 by Elsevier Science Inc. All rights reserved.

**Key Words:** Vertebral trabecular bone; Aging; Osteoporosis; Microstructural model; Mechanical properties; Finite element analysis.

## Introduction

The prevalence of vertebral fractures increases markedly with age.<sup>27</sup> Clinical evidence indicates that an individual's risk of sustaining a vertebral fracture in the future increases as the bone mineral density in their spine decreases,<sup>21,43,44</sup> which is consistent with the strong dependence of vertebral failure load on bone density *ex vivo*.<sup>6,18,28,31</sup> Density reductions in the spine are due primarily to loss of vertebral trabecular bone,<sup>21,37</sup> and reductions in the density<sup>9,31</sup> and strength<sup>33</sup> of vertebral trabecular bone are strongly correlated with reductions in vertebral failure load. Therefore, the physical changes in vertebral trabecular bone that occur with aging, and the effect that these changes have on bone strength, are of particular relevance to the problem of age-related vertebral fractures.

Changes in the microstructure of vertebral trabecular bone with aging have been quantified by histomorphometric analysis, and include reductions in trabecular thickness (Tb.Th) and number (Tb.N).<sup>5,29,51</sup> (Where appropriate, we use the standard nomenclature for trabecular bone histomorphometry as described by Parfitt et al.<sup>39</sup>) Both of these changes are strongly correlated with reductions in bone volume (BV/TV), and represent the two fundamental changes in microstructure associated with reduced bone volume.<sup>5,38,51</sup> Other observed changes in the microstructure of vertebral trabecular bone, such as increased trabecular length<sup>29</sup> and decreased connectivity,<sup>16</sup> are also strongly correlated with changes in bone volume, but can be considered secondary to reductions in the number of trabeculae.<sup>10,35</sup>

It is well established that the mechanical properties of trabecular bone depend strongly on its density or bone volume.<sup>7,42</sup> Because changes in the thickness and number of trabeculae directly affect the bone volume of vertebral trabecular bone, these changes must also affect its mechanical properties. However, the relative effects of reductions in the thickness and number of trabeculae on the mechanical properties of vertebral trabecular bone are not known. Similarly, the importance of both longitudinal and transverse trabeculae in resisting the longitudinal forces acting on the spine has been widely recognized.<sup>4,51</sup> But the relative effects on bone strength of reductions in the thickness and number of longitudinal trabeculae, vs. reductions in the thickness and number of transverse trabeculae, are not known.

Treatment of age-related bone loss using drug therapy has the potential to decrease the incidence of vertebral fractures. However, there has been no direct evidence that drug therapy can increase the number of trabeculae in humans, and the consensus is that resorbed trabeculae cannot be replaced or regenerated.<sup>26,30,38</sup> For example, treatment with parathyroid hormone

Address for correspondence and reprints: Matthew J. Silva, Ph.D., Department of Orthopaedic Surgery, Washington University, One Barnes Hospital Plaza, Suite 11300 West Pavilion, St. Louis, MO 63110. E-mail: silvam@wudosis.wustl.edu

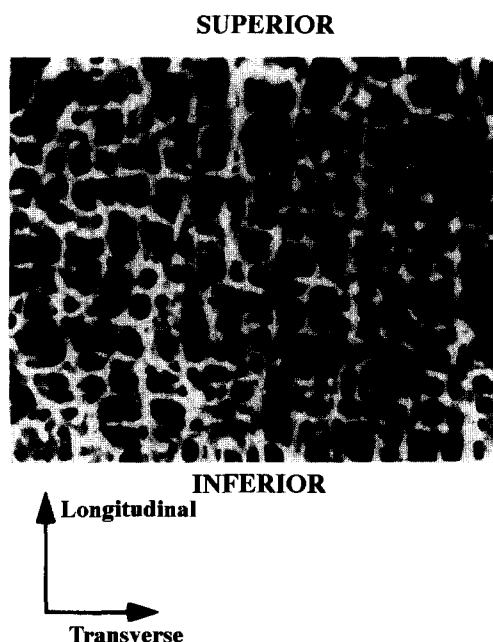


**Figure 1.** Contact radiograph of the central region of a 1-mm-thick, midsagittal section of human vertebral body from a relatively young donor (47-year-old female). The endpoints of each trabecula were digitized and the distribution of trabecular orientation and length were determined for use in developing a two-dimensional microstructural model.

(PTH) in animals has been documented to increase trabecular thickness and bone volume, but not to increase trabecular number.<sup>25,34</sup> While encouraging data on the positive effects of several drug therapies on the strength of trabecular bone in animals have been reported,<sup>3,24,25,32</sup> such data are difficult to obtain in humans. To date, little is known about the effects on mechanical properties of increased bone volume in human vertebral trabecular bone following treatment for age-related bone loss.

Our objective was to develop a microstructural model that was representative of vertebral trabecular bone from humans. Using finite element analysis, the mechanical properties of the model were determined, and the following questions were addressed: What are the effects on modulus and strength of independent reductions in the thickness and number of trabeculae? What are the effects of such changes in the longitudinal vs. transverse directions? What are the effects on modulus and strength of increased trabecular thickness in a model of aged (osteopenic) bone?

## Materials and Methods

Information on trabecular microstructure was collected from 1-mm-thick midsagittal sections of four human vertebral bodies (females, ages 47, 55, 85, and 86 years). Averaged data from these sections, along with data from the literature, provided a basis for the generation of a two-dimensional model of vertebral trabecular bone. The vertebral sections were embedded in methacrylate and contact radiographs were obtained (**Figure 1**) and projected onto a digitizing tablet. The endpoints of each trabecula that was clearly visible within the centrum were digitized (approximately 2000 trabeculae per section), and the trabecular length and orientation (angle from the transverse axis)

were computed. Distributions of the length and orientation of trabeculae were determined.

A two-dimensional finite element model of vertebral trabecular bone was generated using a technique based on Voronoi diagrams. We recently used this technique to develop microstructural models of generic, two-dimensional cellular solids,<sup>47,48</sup> and have since modified it to be more specific for vertebral trabecular bone. A Voronoi diagram is a widely used geometric construction that defines how space in two or three dimensions can be partitioned into cells.<sup>36</sup> A Voronoi diagram is constructed from a set of nucleation points, which may be regularly or randomly spaced. Each cell wall is defined as being equidistant from a pair of adjacent nucleation points. Thus, in the Voronoi diagram, the cell walls bound all points in space which are closer to a single nucleation point than to any other. For our Voronoi diagrams of trabecular bone, the nucleation points did not have a physical significance, but were merely construction entities that allowed us to create diagrams in a repeatable fashion.

A two-dimensional array of  $20 \times 20$  points spaced  $1 \times 1$  mm apart was generated and used as the starting basis for generation of all subsequent diagrams (**Figure 2A**). The coordinates of the points in the square array were perturbed in each direction by a random amount on the range  $-0.3$  to  $0.3$  mm, based on a list of computer-generated, uniformly distributed random numbers.<sup>40</sup> A Voronoi diagram was then generated from the array of perturbed nucleation points (**Figure 2B**) using FORTRAN computer software we developed. To create a model with the appropriate bone

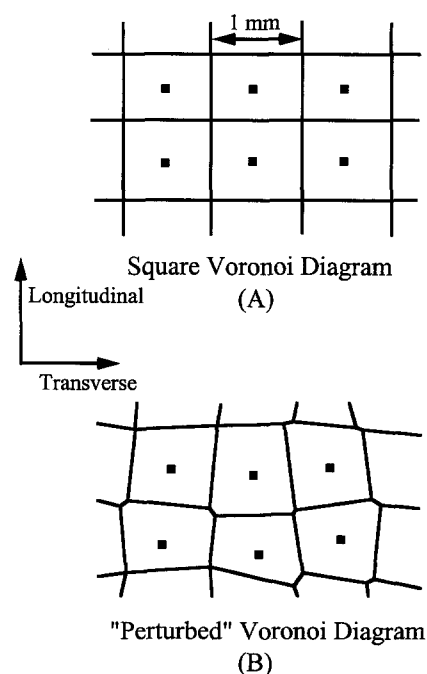


**Figure 2.** Construction of Voronoi diagrams. (A) Portion of square array of nucleation points with spacing  $1 \times 1$  mm. The Voronoi diagram for these nucleation points is generated by constructing the perpendicular bisectors of each pair of adjacent points, and consists of lines that form a square array. The resulting cells are those that would be formed if they began simultaneously from the nucleation points and grew at a uniform rate until contacting the adjacent cells. (B) The nucleation points originally in the square array are perturbed by a random amount in the range  $-0.3$  to  $0.3$  mm. The resulting Voronoi diagram consists of a majority of lines that are oriented within  $\pm 20^\circ$  of the transverse or longitudinal directions, and thus correspond to either the longitudinal or transverse trabeculae that characterize vertebral trabecular bone.

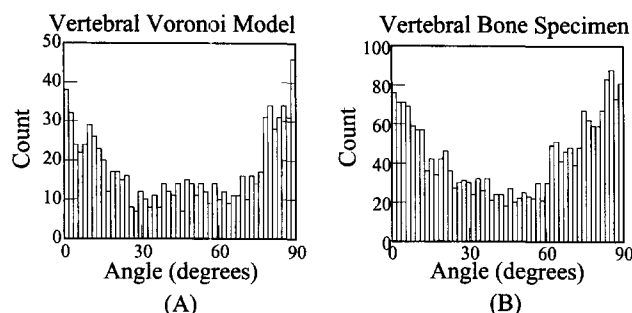


**Figure 3.** Histogram of orientation of cell walls (trabeculae) for a (A) two-dimensional microstructural model of vertebral trabecular bone and a (B) thin section of bone from human vertebral body (Figure 1). 0° corresponds to the transverse direction and 90° to the longitudinal direction. For both the model and the bone section, most cell walls are oriented nearly in the transverse or longitudinal directions.

volume (BV/TV; equal to the area fraction of solid in two dimensions) and degree of anisotropy, the Voronoi diagram (trimmed to approximately  $17 \times 17$  cells) was scaled by 2.33 times in the transverse direction and 3.5 times in the longitudinal direction. The distributions of the orientation and length of trabeculae in the resulting diagrams were comparable to those observed in the vertebral bone sections (Figure 3), and the ratio of the average longitudinal to transverse length (1.15) for the diagrams was comparable to the ratio measured from the sections (1.05). (Longitudinal trabeculae were defined as those  $>45^\circ$  to the transverse axis, whereas transverse trabeculae were  $\leq 45^\circ$ .) Similarly, the ratio of the number of longitudinal to transverse trabeculae (approximately 1.5) was equal to that reported based on two-dimensional histomorphometry of vertebral trabecular bone.<sup>50</sup> [We refer to the “number of trabeculae” as an absolute count of the number of trabeculae in a region of interest; this is not identical to “trabecular number” (TB.N), which is a measure of the number of trabeculae normalized by length of scan line.] Each Voronoi diagram was then converted into a finite element mesh for subsequent analysis of its elastic and ultimate mechanical properties (Figure 4). Each trabecula was modeled as a series of one to three beam elements, depending on its length. Three-noded, quadratic displacement beam elements that included bending, shear, and axial displacement terms were used. A convergence study indicated that the resulting meshes were sufficiently refined to model accurately the nonlinear elastic and failure behaviors of the trabecular structures. Specifically, further increasing the number of elements in the mesh by one third resulted in no difference in the predicted modulus of the structure and only a 2% decrease in predicted failure stress.

Three “intact” finite element meshes were first generated and analyzed. Each mesh was generated using a unique list of random numbers to perturb the nucleation points. Values of 0.213 and 0.153 mm were assigned to the trabecular thicknesses (Tb.Th) in the longitudinal and transverse directions, respectively. The resulting bone volume for each intact mesh was 0.134. The thickness and bone volume values matched the average values for young (average age 29 years) vertebral trabecular bone reported by Mosekilde.<sup>29</sup> The solid, trabecular material was assumed to be isotropic, elastic-perfectly plastic, with a Young’s modulus ( $E_s$ ) of 1.0 MPa, a Poisson’s ratio ( $\nu_s$ ) of 0.3, and a yield strength ( $\sigma_{ys}$ ) of 0.01 MPa. [Following the terminology used for cellular solids,<sup>15</sup> the properties of the solid phase of the models (i.e., the bone) are denoted by a subscript, “s,” and the effective properties

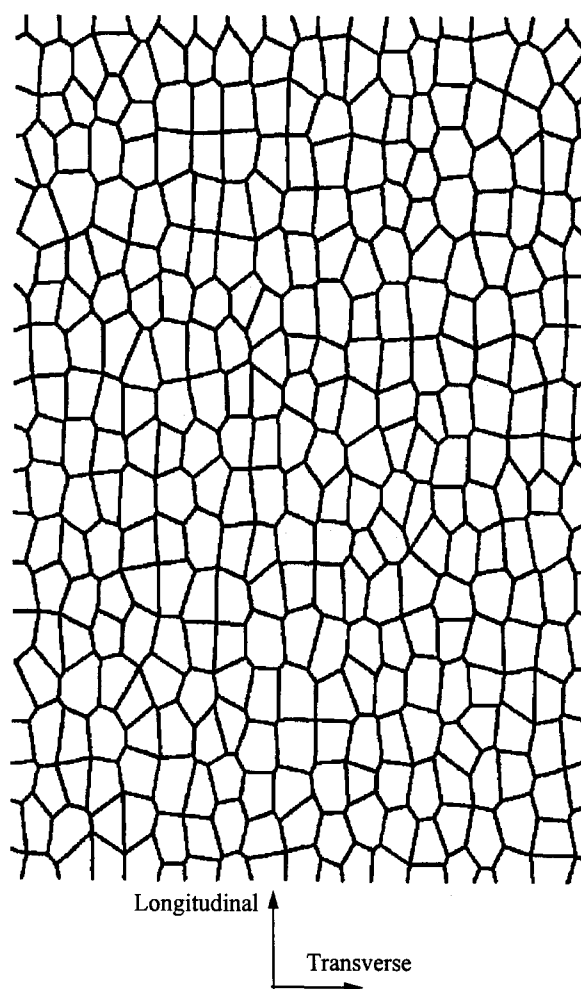


**Figure 4.** Finite element mesh of a model of vertebral trabecular bone. Meshes were comprised of approximately  $17 \times 17$  cells, with the trabeculae modeled by approximately 2500 beam elements. For the “intact” case (as shown), the meshes were assumed to be perfectly connected with no missing trabeculae, and to approximate the appearance of a thin section of vertebral trabecular bone from a relatively young individual (Figure 1).

of the models are denoted by an asterisk, “\*.” Effective properties (sometimes called “apparent” properties) refer to the properties of the model as a whole.] Because all results are presented in dimensionless terms (i.e., as normalized quantities), and because there is considerable uncertainty on the appropriate values of modulus and strength for trabecular material,<sup>2,8,45</sup> the value of modulus was chosen simply for convenience; the ratio of yield strength to modulus (0.01) was chosen as appropriate for compact bone tissue.<sup>41</sup>

The relative modulus ( $E^*/E_s$ ) and strength ( $\sigma^*/\sigma_{ys}$ ) of the finite element meshes were determined for both transverse and longitudinal loading. Displacement boundary conditions simulating uniaxial compression testing to failure (with no friction) were imposed. The analyses allowed for both nonlinear, large displacement (i.e., buckling), and strain softening behaviors, and were performed on a computer workstation (SPARCstation 20, Sun Microsystems, Mountain View, CA) using commercial finite element software (ABAQUS 5.4; Hibbit, Karlsson & Sorensen, Inc., Pawtucket, RI). The modulus of each mesh ( $E^*$ ) was computed as the ratio of normal stress to normal strain in the direction of loading at the first displacement increment (which

**Table 1.** Parameter values for independent changes in the thickness and number of trabeculae for a two-dimensional finite element model of vertebral trabecular bone

Reduction in bone volume (%)	Bone volume (BV/TV)	Longitudinal thickness (Tb.Th) <sub>L</sub> (mm)	Transverse thickness (Tb.Th) <sub>T</sub> (mm)	Number of longitudinal trabeculae	Number of transverse trabeculae
(Intact) 0	0.134	0.213	0.153	563	380
5	0.127	0.196	0.125	516	305
10	0.121	0.182	0.102	483	248
15	0.114	0.167	0.075	446	182

Three different intact meshes, representing bone from young individuals, were first generated and analyzed. Reductions in bone volume from 5%–15% were then prescribed for each of these meshes. The specific values of thickness and number corresponding to each value of bone volume varied slightly for each of the three meshes because of small differences in their microstructures. The values shown are for one of the three meshes. The “number of trabeculae” is an absolute count of the number of trabeculae in a mesh. Because transverse trabeculae contributed only approximately one third to the bone volume of the intact case, larger absolute changes in transverse thickness and number were necessary to produce equivalent reductions in bone volume compared to changes in longitudinal thickness and number.

corresponded to the initial slope of the stress-strain curve), and strength ( $\sigma^*$ ) was defined as the maximum value of stress during the simulated compression test.

The sensitivity of modulus and strength to changes in trabecular microstructure was investigated by independently reducing the thickness and number of trabeculae in each of the two directions (Table 1). Each of the four parameters (longitudinal thickness, longitudinal number, transverse thickness, transverse number) was reduced by an amount necessary to produce reductions in bone volume of 5%, 10%, and 15%, while holding the other three parameters at their intact values. Trabecular thicknesses were reduced uniformly, whereas the numbers of trabeculae were reduced by randomly removing trabeculae from the intact meshes. These parameter changes were performed on the three different intact meshes. Thus, a total of 36 cases were analyzed (3 intact meshes  $\times$  4 parameters  $\times$  3 values of bone volume). Residual values for modulus ( $E^*/E_o^*$ ) and strength ( $\sigma^*/\sigma_o^*$ ) were computed by dividing the modulus and strength of meshes with reduced bone volume by the values for the corresponding intact meshes (i.e.,  $E_o^*$  and  $\sigma_o^*$ ). Thus, each intact mesh served as its own control. Results are reported as the average residual values for the three sets of meshes. Because loading in the longitudinal direction is more physiologically relevant than transverse loading, results are reported primarily for the longitudinal direction.

Two additional analyses were performed, one to simulate aging and one to simulate a possible scenario for restoration of bone mass following the treatment of aged bone. To simulate the aging process, concurrent changes in the number and thickness of both longitudinal and transverse trabeculae were made to an intact mesh (Table 2). Our goal was to generate an “aged” mesh that had a residual strength in the longitudinal direction of approximately 0.2, equal to the ratio between the strengths of old (mean age 81 years) and young (mean age 29) vertebral trabecular bone reported by Mosekilde.<sup>29</sup> The appropriate relative decreases in the number and thickness of trabeculae were determined based on a series of preliminary analyses.<sup>46</sup> The relative

decreases in thickness of the longitudinal and transverse trabeculae were in proportion to the age-related changes reported by Mosekilde. The number of trabeculae were reduced (by random removal) by equal proportions in the two directions to maintain the ratio of longitudinal to transverse numbers at approximately 1.5. The resulting mesh, with its random pattern of defects, qualitatively resembled the appearance of thin sections of vertebral trabecular bone taken from old donors (Figure 5). We then simulated a scenario for the restoration of bone mass following drug treatment of aged bone, in which trabecular thickness increases without changes in the number of trabeculae. In this mesh of “treated” bone, we increased the thicknesses of the longitudinal and transverse trabeculae (by the same relative proportions as they had been decreased to create the aged mesh) to restore bone volume to its intact value, while holding the number of trabeculae fixed at their aged values. The resulting longitudinal and transverse thicknesses were greater than the corresponding intact values because there were fewer trabeculae in the treated mesh than in the intact mesh. The modulus and strength of this treated mesh were determined and compared to the values for the intact and aged bone meshes.

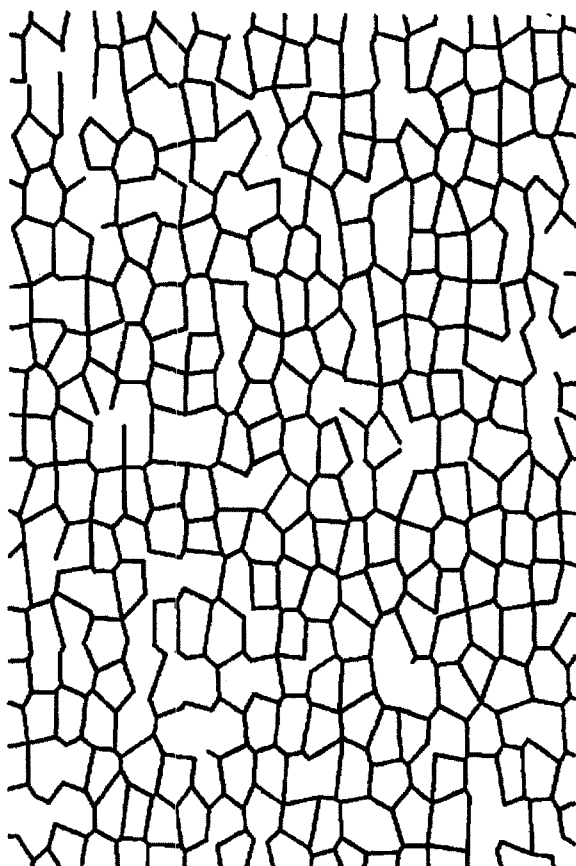
## Results

The compressive stress-strain behavior predicted using the finite element model was comparable to that observed experimentally for specimens of trabecular bone from the human vertebral body (Figure 6). Initial linear elastic behavior was followed by yielding, with stress increasing to a peak value, followed by decreasing stress with further increases in strain (i.e., strain softening). The ratio of strengths in the longitudinal to transverse directions ( $\sigma_L^*/\sigma_T^*$ ) was approximately 2.1, which is comparable to the anisotropy ratio reported for young (average age 29 years) vertebral trabecular bone.<sup>29</sup> The physical basis for the strain softening behavior was the localized collapse of two to three adjacent rows of cells (Figure 7). This localization of deformation was similar to that observed in sections of vertebral trabec-

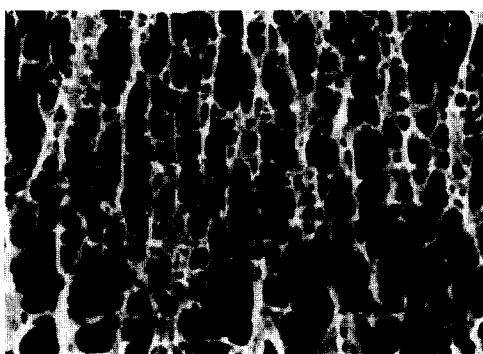
**Table 2.** Microstructural parameters for simulation of aging and drug treatment in a two-dimensional model of vertebral trabecular bone

Case	Bone volume (BV/TV)	Longitudinal thickness (Tb.Th) <sub>L</sub> (mm)	Transverse thickness (Tb.Th) <sub>T</sub> (mm)	Number of longitudinal trabeculae	Number of transverse trabeculae
Intact	0.134	0.213	0.153	563	380
Aged	0.114	0.207	0.134	502	338
Treated	0.134	0.225	0.190	502	338

The *intact* case is the same as described in Table 1, and represents a relatively young condition. The *aged* case simulates the concurrent reduction of the thickness and number of trabeculae in both longitudinal and transverse directions that occurs with aging. The *treated* case simulates the restoration of bone volume by increasing the thickness of the trabeculae that remain after aging.



SUPERIOR



INFERIOR

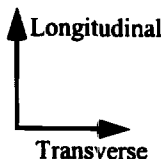


**Figure 5.** (A) Finite element mesh of "aged" vertebral trabecular bone. Approximately 11% of the trabeculae have been removed at random from an initially intact mesh (Figure 3) and the thickness of the trabeculae have also been reduced (not shown). (B) Contact radiograph of a 1-mm-thick, midsagittal section of a human vertebral body from relatively old donor (85-year-old female). The random pattern of defects is qualitatively represented by the missing trabeculae of the aged mesh.

ular bone following compressive failure.<sup>49</sup> The unloading response of the models (not shown) indicated that both elastic and permanent deformations contributed to cell collapse, which is evidence that both elastic buckling and plastic collapse failure modes were present.

Modulus and strength were approximately two to five times more sensitive to reductions in the number of trabeculae than to reductions in trabecular thickness that produced the same decrease in bone volume (Figure 8). For example, randomly removing longitudinal trabeculae to achieve a 10% reduction in bone volume reduced the residual strength to 0.30, whereas removing the same amount of bone by uniformly reducing the thickness of the longitudinal trabeculae only lowered the residual strength to 0.80. Reductions in the thickness or number of transverse trabeculae caused reductions in modulus and strength that were comparable to the reductions caused by bone volume-equivalent changes in the longitudinal trabeculae. For example, reducing the number of transverse trabeculae to achieve a 10% reduction in bone volume reduced the residual strength to 0.37, compared to a residual strength of 0.30 following a bone volume-equivalent reduction in the number of longitudinal trabeculae. Thus, changes in transverse trabeculae had important consequences on mechanical properties, even for loading in the longitudinal direction.

Concurrent reductions in the thickness and number of both transverse and longitudinal trabeculae were implemented to simulate the effects of aging on vertebral trabecular bone. The residual modulus and strength of the aged case (relative to the intact case) were 0.18 and 0.23, respectively (Figure 9). When trabecular thickness was increased to restore the bone volume of the aged case to that of the intact case, without restoring the number of trabeculae, the residual modulus and strength increased to only 0.32 and 0.37, respectively. Thus, the treated case was approximately 60% stronger than the aged case, but only 37% as strong as the intact case.

## Discussion

A two-dimensional, microstructural model of human vertebral trabecular bone was developed and analyzed using finite element

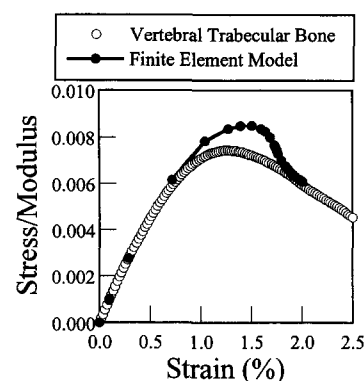


**Figure 6.** Comparison of compressive stress-strain curves for vertebral trabecular bone (as determined by mechanical testing of human specimens<sup>23</sup>) and for a microstructural model of vertebral trabecular bone (as determined by finite element analysis). Because two-dimensional models typically underestimate the absolute properties of three-dimensional materials, and because the absolute tissue properties for trabecular bone are uncertain, stress is normalized by modulus to allow for a comparison on the same scale. The model correctly predicts the qualitative behavior of trabecular bone, including the initial, elastic behavior, followed by yielding and subsequent strain softening.

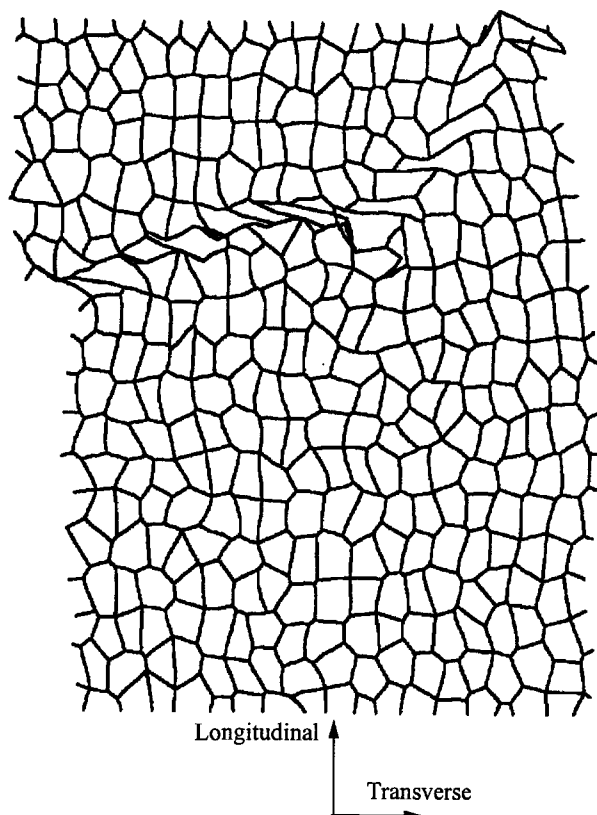


**Figure 7.** Deformed state of a vertebral trabecular bone model due to loading in the longitudinal direction. The development of a highly localized failure band was characteristic of the failure mode of all the cases, and for loading in both directions. This pattern compares favorably to the observed failure mode of vertebral trabecular bone in compression.

analysis. Its predicted stress-strain behavior and failure mode were comparable to those observed for vertebral trabecular bone under compressive loading. The modulus and strength of the model were at least twice as sensitive to random reductions in the *number* of trabeculae as compared to bone volume-equivalent, uniform reductions in the *thickness* of trabeculae. The modulus and strength (in the longitudinal direction) were approximately as sensitive to microstructural changes affecting the transverse trabeculae as to changes affecting the longitudinal trabeculae. For a case simulating aged bone, in which the thickness and number of trabeculae were reduced concurrently, the modulus and strength were approximately 20% of their values for the intact (young) case. When a treatment that restores bone mass was simulated by increasing the thickness, but not the number, of trabeculae, the modulus and strength increased by 60% and 75%, respectively, compared to the aged case, but were still less than 40% of the values for the intact case.

The approach we used to model vertebral trabecular bone has several strengths. First, the important microstructural features of vertebral trabecular bone were replicated. These include the characteristic arrangement of trabeculae in either longitudinal or transverse orientations,<sup>1</sup> with the longitudinal trabeculae being thicker and slightly longer than the transverse trabeculae.<sup>29</sup> These microstructural features dictated that the models behave anisotropically, consistent with the behavior of vertebral trabecular bone. Despite the predominant transverse or longitudinal arrangement of trabeculae, their overall pattern was sufficiently random relative to the direction of loading that bending occurred

in many of the trabeculae. In fact, bending was the predominant mode of deformation within the trabecular network, which is consistent with the power-law relation that has been observed between density and the mechanical properties of vertebral trabecular bone.<sup>14,17,22</sup> To provide further evidence that our models were appropriate for analyzing the behavior of vertebral trabecular bone, we compared the distribution of local strains in our model to the distributions reported by Wenzel et al.<sup>55</sup> based on their analysis of specimens of vertebral trabecular bone. Excellent agreement between the two distributions was observed (**Figure 10**). In addition, our model data closely fit the probability density function that Fyhrie and coworkers<sup>12,55</sup> have suggested is most appropriate for describing the distribution of strain in specimens of vertebral trabecular bone loaded in unconfined compression.

A second strength of this study is that we modeled vertebral trabecular bone in a generic fashion, rather than modeling the

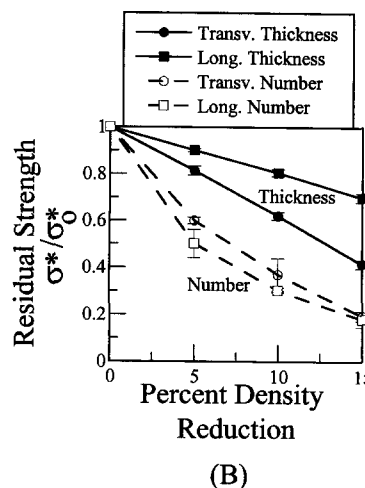
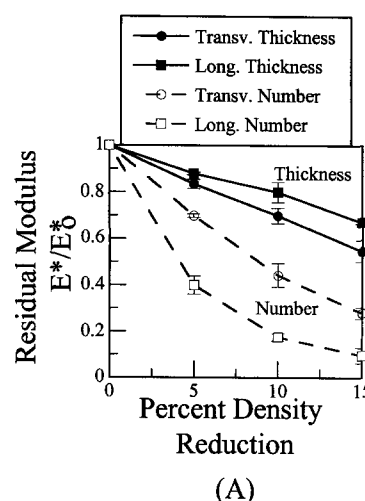


**Figure 8.** Residual modulus (A) and strength (B) in the longitudinal direction for four different modes of bone volume reduction. Modulus and strength are presented as residual values, normalized by the values corresponding to zero reduction in bone volume. Each data point is the mean value from three different finite element meshes; error bars denote 1 standard deviation (where not shown, standard deviations were less than 0.02). Modulus and strength were at least twice as sensitive to changes in the number of trabeculae as to changes in the thickness of trabeculae. Comparable findings were observed for loading in the transverse direction.

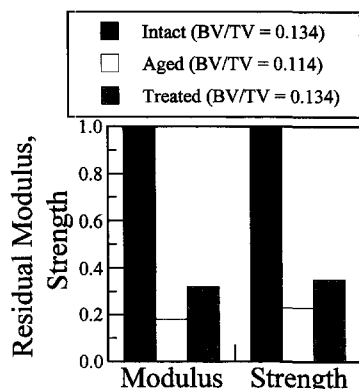


**Figure 9.** Modulus and strength for finite element meshes of intact, aged, and treated vertebral trabecular bone. In the intact case, the trabecular network is fully connected and the trabeculae are relatively thick (Figure 4); in the aged case, both the thickness and number of trabeculae have been reduced, simulating age-related changes in trabecular microstructure (Figure 5A); in the treated mesh, the bone volume has been increased to its intact level by increasing trabecular thickness, but the number of trabeculae is the same as for the aged case. Results are presented as residual values, normalized by the values for the intact case. The aged case had only approximately 20% of the modulus and strength of the intact case. The mechanical properties of the treated case were increased relative to the aged case, but were still less than 40% of the properties of the intact case.

specific microstructure of individual specimens of bone. An analogous approach was described by Jensen et al.,<sup>20</sup> who created a generic model of vertebral trabecular bone based on some of the same histomorphometric data that we used. The elastic behavior of their model qualitatively matched the behavior of experimentally tested specimens of bone, and illustrated the utility of a simplified model to understand relations between microstructure and mechanical properties. Such generic models represent a complementary approach to more anatomically accurate, specimen-specific modeling of vertebral trabecular bone. While the analysis of trabecular bone specimens whose microstructures are modeled in precise detail<sup>12,19,53,55</sup> has merit in helping to understand structure-property relations, results from such models are often difficult to generalize. Because we analyzed a generic model of vertebral trabecular bone, our results are not based solely on the microstructure of a particular specimen. Once the modeling procedures were established, a number of generic meshes, each with a unique microstructure, were easily created and analyzed, allowing average behaviors to be reported. Because of the relatively small numbers of elements in our meshes, we were able to analyze both elastic and failure behaviors. To date, most specimen-specific models have been limited to elastic analyses because of the large numbers of elements involved and the related computational difficulties. A third strength of this study is that trabecular microstructure could be varied in a controlled fashion, and thus the effects of independent variations in microstructure on mechanical properties were readily investigated. Because several concurrent changes in the microstructure of vertebral trabecular bone occur with aging,<sup>29</sup> it is difficult to establish the relative effects of each of these changes independently, either by specimen-specific, microstructural finite element analysis, or by histomorphometric analysis combined with mechanical testing. The approach developed in this study is ideally suited to estimating the relative effects of such changes.

Several limitations should also be noted. First, we assumed trabecular thickness to be uniform, with one value for all longi-

tudinal trabeculae and a second value for all transverse trabeculae. Thus, we did not account for the natural variance in trabecular thickness present in vertebral trabecular bone. Variations in the trabecular thickness of the initial model would likely result in reduced modulus and strength compared to the uniform thickness case.<sup>48,54</sup> Similarly, if we reduced trabecular thickness nonuniformly rather than uniformly, we probably would have observed a greater decrease in strength for a given decrease in bone volume. Nonetheless, we expect that any physiological pattern of trabecular thinning would cause less of a decrease in the effective mechanical properties than a bone volume-equivalent reduction in the number of trabeculae. A second limitation is that we removed trabeculae randomly rather than based on any initial state of stress or strain, or based on any initial distribution of trabecular thickness. As a result, we may have overestimated the effects of trabecular removal on mechanical properties if resorption preferentially removes thinner and/or less heavily loaded trabeculae. But, because the factors governing activation of local resorption in trabecular bone are not clearly defined, we chose to use an unbiased strategy for removing trabeculae. Histomorphometric data on human vertebral trabecular bone indicate that age-related changes in microstructure are consistent with a pattern of random deletion of trabeculae,<sup>13</sup> which supports the validity of our approach.

Another important limitation is that our model was a two-dimensional representation of a three-dimensional material. Thus, no direct comparisons could be made between absolute values of modulus or strength predicted using our model and those measured on bone specimens experimentally. Another consequence of using a two-dimensional model is that the mechanical properties were more sensitive to reductions in the thickness and number of trabeculae than would be expected for a three-dimensional model of vertebral trabecular bone. Based on unit cell analyses of cellular materials, the mechanical properties depend on cell wall thickness as a power law function; the exponent of the function is greater for two-dimensional models

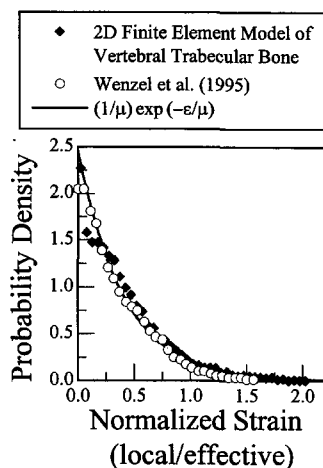


**Figure 10.** Probability density of the local (trabecular level) strain magnitude normalized by the effective strain for compressive loading of a finite element model of vertebral trabecular bone. Axial strains (i.e., along the local trabecular axis) were sampled on both surfaces of the beam elements at each finite element node. The model findings closely matched the probability density data reported by Wenzel et al.<sup>55</sup> based on a detailed, specimen-specific finite element model of a specimen of vertebral trabecular bone loaded in unconfined compression. The data also closely fit a probability density function of the form:  $(1/\mu)\exp(-\epsilon/\mu)$ , where  $\epsilon$  is the normalized strain magnitude, and  $\mu$  is the mean value of  $\epsilon$  ( $\mu = 0.405$ ;  $r^2 = 0.96$ ).

than for analogous three-dimensional models.<sup>14</sup> Similarly, because two-dimensional networks have fewer connections, on average, at each node than three-dimensional networks, the structural consequences of losing a given proportion of connections (i.e., reducing the number of branches or trabeculae) are greater for a two-dimensional network than for a three-dimensional network. Results based on percolation theory<sup>52</sup> suggest that the mechanical properties of a two-dimensional network having an average of three branches per node will degrade to zero (i.e., residual modulus and strength equal to zero) when approximately one third of its branches are removed, a finding that has been confirmed computationally.<sup>11,47</sup> By comparison, the properties of a three-dimensional network having four branches per node will degrade to zero when approximately one-half of its branches are removed. Taken together, these comparisons suggest that reducing the thickness and number of trabeculae to achieve a given reduction in bone volume in a three-dimensional model of vertebral trabecular bone would cause reductions in the mechanical properties less than those we report based on our two-dimensional model. Research on the structural consequences of thinning and removal of trabeculae from three-dimensional models of bone is needed to further investigate this issue, and to determine if the relative importance of trabecular thickness vs. number is consistent with our current findings.

The findings of this study have relevance to the study of failure mechanisms in trabecular bone. The marked reductions in strength of the bone models caused by reductions in the number of transverse trabeculae are consistent with failure by buckling of the longitudinal trabeculae.<sup>46</sup> Reductions in the number of transverse trabeculae increase the average, unsupported length of longitudinal trabeculae, and make them more susceptible to buckling failure. Buckling failure has been recognized previously as being of relevance to the failure of vertebral trabecular bone,<sup>4,51</sup> and our results support the concept that the buckling failure of longitudinal trabeculae, caused by loss of transverse trabeculae, is an important factor in the age-related loss of vertebral bone strength.

Finally, the results of this study have clinical relevance with regard to the treatment of age-related bone loss. Treatment strategies can be described as either *prevention* (i.e., initiated before bone loss has occurred) or *intervention* (i.e., initiated after bone loss has occurred). In this context, our simulation of aging and treatment investigated the scenario in which intervention was initiated after advanced bone loss had occurred and the bone had lost 80% of its initial strength. For the optimistic case of a full recovery of bone mass, the strength was increased by approximately 60% compared to its pretreatment value (Figure 9). However, the strength was still only one third of its initial (young) value, because the treatment did not increase the number of trabeculae. Thus, after a period of advanced bone loss, intervention treatment did not restore bone to its initial strength in our two-dimensional model of vertebral trabecular bone. Our findings support the view that, until treatments exist that can increase trabecular number, the most effective treatment strategy is to prevent the degradation of bone strength by maintaining the number of trabeculae at a healthy level. This could be done by starting a course of prevention treatment shortly after peak bone mass is achieved.

(AR41894-0182), by the Maurice E. Mueller Professorship in Biomechanics at Harvard Medical School, and the Harry and Evelyn Indursky and family Orthopedic Biomechanics Laboratory at Beth Israel Deaconess Medical Center.

## References

1. Arnold, J. S. External and trabecular morphologic changes in lumbar vertebrae with aging. Conference proceedings: Progress in methods of bone measurement. Bethesda, MD: US Dept. of Health, Education and Welfare; 352–411; 1970.
2. Ashman, R. B. and Rho, J. Y. Elastic modulus of trabecular bone material. *J Biomech* 21:177–181; 1988.
3. Balena, R., Toolan, B. C., Shea, M. et al. The effects of 2-year treatment with the aminobisphosphonate alendronate on the bone metabolism, bone histomorphometry, and bone strength in ovariectomized nonhuman primates. *J Clin Invest* 92:2577–2586; 1993.
4. Bell, G. H., Dunbar, O., Beck, J. S., and Gibb, A. Variations in strength of vertebrae with age and their relation to osteoporosis. *Calcif Tissue Res* 1:75–86; 1967.
5. Bergot, C., Laval-Jeantet, A., Preteux, F., and Meunier, A. Measurement of anisotropic vertebral trabecular bone loss during aging by quantitative image analysis. *Calcif Tissue Int* 43:143–149; 1988.
6. Brinckmann, P., Biggemann, M., and Hilweg, D. Prediction of the compressive strength of human lumbar vertebrae. *Spine* 14:606–610; 1989.
7. Carter, D. R. and Hayes, W. C. The compressive behavior of bone as a two-phase porous structure. *J Bone Jt Surg* 59-A:954–962; 1977.
8. Choi, K., Kuhn, J. L., Ciarelli, M. J., and Goldstein, S. A. The elastic moduli of human subchondral, trabecular, and cortical bone tissue and the size-dependency of cortical bone modulus. *J Biomech* 23:1103–1113; 1990.
9. Cody, D. D., Goldstein, S. A., Flynn, M. J., and Brown, E. B. Correlations between vertebral regional bone mineral density (rBMD) and whole bone fracture load. *Spine* 16:146–154; 1991.
10. DeHoff, R. T. Curvature and the topological properties of interconnected phases. In: DeHoff, R. T. and Rhines, F. N., Eds. *Quantitative Microscopy*. New York: McGraw-Hill; 1968; 291–325.
11. Duxbury, P. M., Kim, S. G., and Leath, P. L. Size effect and statistics of fracture in random materials. *Mater Sci Eng A* 176:25–31; 1994.
12. Fyhrie, D. P. and Hamid, M. S. The probability distribution of trabecular level strains for vertebral cancellous bone. *Trans Orthop Res Soc* 18:175; 1993.
13. Fyhrie, D. P., Lang, S. M., Hoshaw, S. J., Schaffler, M. B., and Kuo, R. F. Human vertebral cancellous bone surface distribution. *Bone* 17:287–291; 1995.
14. Gibson, L. J. The mechanical behavior of cancellous bone. *J Biomech* 18:317–328; 1985.
15. Gibson, L. J. and Ashby, M. F. *Cellular Solids: Structures and Properties*. Oxford: Pergamon; 1988.
16. Goldstein, S. A., Goulet, R., and McCubbrey, D. Measurement and significance of three-dimensional architecture to the mechanical integrity of trabecular bone. *Calcif Tissue Int* 53(Suppl.):S127–S133; 1993.
17. Hansson, T. H., Keller, T. S., and Panjabi, M. M. A study of the compressive properties of lumbar vertebral trabeculae: Effects of tissue characteristics. *Spine* 12:56–62; 1987.
18. Hansson, T., Roos, B., and Nachemson, A. The bone mineral content and ultimate compressive strength of lumbar vertebrae. *Spine* 5:46–55; 1980.
19. Hollister, S. J., Brennan, J. M., and Kikuchi, N. A homogenization sampling procedure for calculating trabecular bone stiffness and tissue level stress. *J Biomech* 27:433–444; 1994.
20. Jensen, K. S., Mosekilde, L., and Mosekilde, L. A model of vertebral trabecular bone architecture and its mechanical properties. *Bone* 11:417–423; 1990.
21. Johnston, C. C. and Melton, L. J. Bone densitometry. In: Riggs, B. L. and Melton, L. J., Eds. *Osteoporosis: Etiology, Diagnosis, and Management*. Philadelphia: Lippincott-Raven; 1995; 275–297.
22. Keller, T. S. Predicting the compressive mechanical behavior of bone. *J Biomech* 27:1159–1168; 1994.
23. Kopperdahl, D. L. and Keaveny, T. M. Yield strain behavior of trabecular bone. *J Biomech*. In press.
24. Lauritzen, D. B., Balena, R., Shea, M. et al. Effects of combined prostaglandin and alendronate treatment on the histomorphometry and biomechanical properties of ovariectomized rats. *J Bone Miner Res* 8:871–879; 1993.
25. Li, M., Mosekilde, L., Sogaard, C. H., Thonsen, J. S., and Wronski, T. J. Parathyroid hormone monotherapy and cotherapy with antiresorptive agents

**Acknowledgments:** The helpful comments of Mary Boussein and Ralph Mueller of the Orthopedic Biomechanics Lab at Beth Israel Deaconess Medical Center and Professor Mary Boyce of MIT are gratefully acknowledged. This study was supported by grants from the National Science Foundation (EID-9023692) and the National Institutes of Health

- restore vertebral bone mass and strength in aged ovariectomized rats. *Bone* 16:629–635; 1995.
26. Melsen, F., Mosekilde, L., Brixen, K., and Steinicke, T. ADFR—the concept and its performance. In: Marcus, R., Feldman, D., and Kelsey, J., Eds. *Osteoporosis*. San Diego: Academic; 1996; 1145–1158.
27. Melton, L. J. Epidemiology of fractures. In: Riggs, B. L. and Melton, L. J., Eds. *Osteoporosis: Etiology, Diagnosis, and Management*. New York: Raven; 1988; 133–154.
28. Moro, M., Hecker, A. T., Bouxsein, M. L., and Myers, E. R. Failure load of thoracic vertebrae correlates with lumbar bone mineral density measured by DXA. *Calcif Tissue Int* 56:206–209; 1995.
29. Mosekilde, L. Sex differences in age-related loss of vertebral trabecular bone mass and structure—biomechanical consequences. *Bone* 10:425–432; 1989.
30. Mosekilde, L. Age-related loss of vertebral trabecular bone mass and structure—biomechanical consequences. In: Mow, V. C., Ratcliffe, A., and Woo, S. L., Eds. *Biomechanics of Diarthrodial Joints*. Berlin: Springer; 1990; 83–96.
31. Mosekilde, L., Bentzen, S. M., Ortoft, G., and Jorgensen, J. The predictive value of quantitative computed tomography for vertebral body compressive strength and ash density. *Bone* 10:465–470; 1989.
32. Mosekilde, L., Danielsen, C. C., and Gasser, J. The effect on vertebral bone mass and strength of long term treatment with antiresorptive agents (estrogen and calcitonin), human parathyroid hormone-(1–38), and combination therapy, assessed in aged ovariectomized rats. *Endocrinology* 134:2126–2134; 1994.
33. Mosekilde, L. and Mosekilde, L. Normal vertebral body size and compressive strength: Relations to age and to vertebral and iliac trabecular bone compressive strength. *Bone* 7:207–212; 1986.
34. Mosekilde, L. and Reeve, J. Treatment with PTH peptides. In: Marcus, R., Feldman, D., and Kelsey, J., Eds. *Osteoporosis*. San Diego: Academic; 1996; 1293–1311.
35. Odgaard, A. and Gundersen, H. J. G. Quantification of connectivity in cancellous bone, with special emphasis on 3-D reconstructions. *Bone* 14:173–182; 1993.
36. Okabe, A., Boots, B., and Sugihara, K. *Spatial Tesselations: Concepts and Applications of Voronoi Diagrams*. Chichester: Wiley; 1992.
37. Pacifici, R., Rupich, R. C., and Avioli, L. V. Vertebral cortical bone mass measurement by a new quantitative computer tomography method: Correlations with vertebral trabecular bone measurements. *Calcif Tissue Int* 47:215–220; 1990.
38. Parfitt, A. M. Implications of architecture for the pathogenesis and prevention of vertebral fracture. *Bone* 13(Suppl.):S41–S47; 1992.
39. Parfitt, A. M., Drezner, M. K., Glorieux, F. H. et al. Bone histomorphometry: Standardization of nomenclature, symbols, and units. *J Bone Miner Res* 2:595–610; 1987.
40. Press, W. H., Teukolsky, S. A., Vetterling, W. T., and Flannery, B. P. *Numerical Recipes in Fortran*. Cambridge: Cambridge University Press; 1992.
41. Reilly, D. T. and Burstein, A. H. The elastic and ultimate properties of compact bone tissue. *J Biomech* 8:393–405; 1975.
42. Rice, J. C., Cowin, S. C., and Bowman, J. A. On the dependence of the elasticity and strength of cancellous bone on apparent density. *J Biomech* 21:155–168; 1988.
43. Ross, P. D., Davis, J. W., Epstein, R. S., and Wasnich, R. D. Pre-existing fractures and bone mass predict vertebral fracture incidence in women. *Ann Intern Med* 114:919–923; 1991.
44. Ross, P. D., Davis, J. W., Vogel, J. M., and Wasnich, R. D. A critical review of bone mass and the risk of fractures in osteoporosis. *Calcif Tissue Int* 46:149–161; 1990.
45. Ryan, S. D. and Williams, J. L. Tensile testing of rodlike trabeculae excised from bovine femoral bone. *J Biomech* 22:351–355; 1989.
46. Silva, M. J. Predicting the Failure Behavior of the Human Vertebral Body. Ph.D. Thesis. Massachusetts Institute of Technology; 1996.
47. Silva, M. J. and Gibson, L. J. The effects of non-periodic microstructure and defects on the compressive strength of two-dimensional cellular solids. *Int J Mech Sci* 39:549–563; 1997.
48. Silva, M. J., Hayes, W. C., and Gibson, L. J. The effects of non-periodic microstructure on the elastic properties of two-dimensional cellular solids. *Int J Mech Sci* 37:1161–1177; 1995.
49. Silva, M. J., Keaveny, T. M., and Hayes, W. C. Computed tomography-based finite element models predict failure load and location of failure in vertebral slices. *Trans Orthop Res Soc* 21:273; 1996.
50. Snyder, B. D. Anisotropic Structure–Property Relations for Trabecular Bone: An analysis of the Morphological and Constitutive Properties of Trabecular Bone from the Human Proximal Femur and Lumbar Spine. Ph.D. Thesis. University of Pennsylvania; 1991.
51. Snyder, B. D., Piazza, S., Edwards, W. T., and Hayes, W. C. Role of trabecular morphology in the etiology of age-related vertebral fractures. *Calcif Tissue Int* 53(Suppl.):S14–S22; 1993.
52. Stauffer, D. and Aharony, A. *Introduction to Percolation Theory*. London: Taylor & Francis; 1992.
53. van Rietbergen, B., Weinans, H., Huiskes, R., and Odgaard, A. A new method to determine trabecular bone elastic properties and loading using micromechanical finite-element models. *J Biomech* 28:69–81; 1995.
54. Wachtel, E. F. and Keaveny, T. M. Intra-specimen variations in trabecular thickness decrease trabecular modulus. *Trans Orthop Res Soc* 22:61; 1997.
55. Wenzel, T. E., Fyhrie, D. P., and Hollister, S. J. A simple mathematical model for strain distributions in cancellous bone. *Trans Orthop Res Soc* 20:537; 1995.

Date Received: August 28, 1996

Date Revised: April 28, 1997

Date Accepted: April 28, 1997